J Comp Physiol A (2015) 201:357–374
DOI 10.1007/s00359-015-0995-6

ORIGINAL PAPER

Comparative histology of the adult electric organ among four species of the genus *Campylomormyrus* (Teleostei: Mormyridae)

Christiane Paul · Victor Mamonekene · Marianne Vater · Philine G. D. Feulner · Jacob Engelmann · Ralph Tiedemann · Frank Kirschbaum

Received: 11 March 2014 / Revised: 19 February 2015 / Accepted: 25 February 2015 / Published online: 10 March 2015

Abstract The electric organ (EO) of weakly electric mormyrids consists of flat, disk-shaped electrocytes with distinct anterior and posterior faces. There are multiple species-characteristic patterns in the geometry of the electrocytes and their innervation. To further correlate electric organ discharge (EOD) with EO anatomy, we examined four species of the mormyrid genus *Campylomormyrus* possessing clearly distinct EODs. In *C. compressirostris*, *C. numenius*, and *C. tshokwe*, all of which display biphasic EODs, the posterior face of the electrocytes forms evaginations merging to a stalk system receiving the innervation. In *C. tamandua* that emits a triphasic EOD, the small stalks of the electrocyte penetrate the electrocyte anteriorly before merging on the anterior side to receive the innervation. Additional differences in electrocyte anatomy among the former three species with the same EO geometry could be associated with further characteristics of their EODs. Furthermore, in *C. numenius*, ontogenetic changes in EO anatomy correlate with profound changes in the EOD. In the juvenile the anterior face of the electrocyte is smooth, whereas in the adult it exhibits pronounced surface foldings. This anatomical difference, together with disparities in the degree of stalk furcation, probably contributes to the about 12 times longer EOD in the adult.

Keywords Mormyridae · *Campylomormyrus* · Electric organ discharge · Electrocyte geometry · Electric organ ontogeny

Introduction

The electric organ (EO) of a mormyrid fish was first described on the basis of *Mormyrus longipinnis* (Rüppel 1832). Since then, many studies have been devoted to the anatomy and physiology of this specialized tissue, which is capable of producing weak electric discharges (Marcusen 1864; Ogneff 1898; Schlichter 1906; Szabo 1956, 1957, 1958; Lissmann 1958; Bennett and Grundfest 1961; Bennett

Electronic supplementary material The online version of this article (doi:10.1007/s00359-015-0995-6) contains supplementary material, which is available to authorized users.

C. Paul · R. Tiedemann
Unit of Evolutionary Biology/Systematic Zoology, Institute of Biochemistry and Biology, University of Potsdam, Karl-Liebknecht-Str. 24-25, Haus 26, 14476 Potsdam-Golm, Germany

V. Mamonekene
Ecole Nationale Supérieure d'Agronomie et de Foresterie, Université Marien Ngouabi, B.P. 69, Brazzaville, Republic of Congo

M. Vater
Unit of General Zoology, Institute of Biochemistry and Biology, University of Potsdam, Karl-Liebknecht-Str. 24-25, Haus 26, 14476 Potsdam-Golm, Germany

P. G. D. Feulner
Department of Fish Ecology and Evolution, Center for Ecology, Evolution and Biogeochemistry, Eawag, Swiss Federal Institute of Aquatic Science and Technology, Seestrasse 79, 6047 Kastanienbaum, Switzerland

J. Engelmann
Faculty of Biology, AG Active Sensing, Bielefeld University, Universitätsstraße 25, 33615 Bielefeld, Germany

F. Kirschbaum (✉)
Unit of Biology and Ecology of Fishes, Faculty of Life Sciences, Humboldt University of Berlin, Philippstr. 13, Haus 16, 10115 Berlin, Germany
e-mail: frank.kirschbaum@staff.hu-berlin.de

1970, 1971; Bruns 1971; Schwartz et al. 1975; Bell et al. 1976; Bass 1986; Bass et al. 1986). Mormyrids utilize their weak electric sense for electrolocation (Von der Emde and Ringer 1992; Von der Emde 1999, 2006), foraging (Von der Emde and Bleckmann 1998; Von der Emde and Schwarz 2002) and social communication (Moller 1970; Hopkins and Bass 1981; Kramer and Kuhn 1994; Kramer 1996).

In adult Mormyridae, the EO is confined to the caudal peduncle of the fish. It is built up of electrocytes, which are apparently derived from skeletal muscle fibers (Szabo 1960, 1961). Detailed ontogenetic studies, however, have shown that the electrocytes of the adult organ differentiate into the adult structure without passing through a typical muscle fiber stage (Kirschbaum 1977, 1982). They are characterized by their flat, disk-shaped appearance resulting in a clear orientation toward the longitudinal body axis (Denizot et al. 1982). Usually, the posterior face of the thin electrocyte possesses a number of evaginations, called stalks, which either fuse into one or several major stalks on their site of origin (posterior) or penetrate the cell and merge at the anterior site to form the major stalk(s) (see Bass 1986 for examples). Each major stalk is innervated by electromotor neurons of the spinal cord, or, more precisely, each major stalk is in contact with numerous synapses of the neuron (Denizot et al. 1982). The stalk induces the activation of the innervated face of the electrocyte by propagating action potentials along its branches (Bennett and Grundfest 1961), whereas the initial command for the activation originates from a command nucleus located in the medulla oblongata (Bell et al. 1983; Grant et al. 1986). However, through joint excitation of all electrocytes, the single cell currents summate to a weak electric field measurable externally from the fish. The waveform of such an electric pulse is called an electric organ discharge (EOD). The waveform and patterning of the EODs are often species specific (Hopkins 1981; Hopkins and Bass 1981; Kramer and Kuhn 1994; Feulner et al. 2008). Consequently, this trait is a useful tool for the identification of otherwise cryptic species (Hopkins 1999), especially since the Mormyridae encompass more than 200 species in 19 genera arisen from an adaptive radiation (Sullivan et al. 2000), which is probably still ongoing.

Bass (1986) introduced the term "electrocyte geometry" to characterize the pattern of electrocyte organization, i.e., presence or absence of a penetrating stalk. His study supported a correlation between a certain electrocyte geometry and the number and polarity of the EOD's phases, as proposed before by Bennett and Grundfest (1961). Five basic electrocyte types with regard to geometry of the stalk system and site of origin of the stalks can be distinguished in mormyrids and each correlates with certain EOD characteristics (reviewed in Hopkins 1999). The site of innervation was found to crucially define the polarity of the first EOD phase (Bennett and Grundfest 1961; Bass 1986). Biphasic EODs, e.g., often correlate with innervation on the posterior face of the electrocyte (non-penetrating stalk, referred to as NP_p type), whereas triphasic EODs are often associated with anterior innervation of the electrocyte (penetrating stalks; referred to as P_a type).

Furthermore, also many other architectural features of the electrocyte (e.g., degree of proliferation of the anterior face, thickness of the electrocyte or size of the stalks) could be explicitly correlated with differences in EOD waveform and duration (Bass 1986; Bass et al. 1986; Freedman et al. 1989; Alves-Gomes and Hopkins 1997). Hence, there are—despite a common general organization of the EO in all members of Mormyridae—numerous aspects in which EOs can be different among and even within species, opening up several areas of research: (1) the diversity of electrocyte fine anatomy (e.g., the organization and structure of anterior and posterior faces or electrocyte geometry; see Bass 1986); (2) EO physiology, i.e., how the EOD is produced is variable even among closely related species (Bennett and Grundfest 1961; Bennett 1971); (3) developmental changes, i.e., EOs can undergo anatomical changes during a species' ontogeny with corresponding changes in EOD waveform and duration (Cheng 2012); (4) sexual dimorphism, i.e., EOs can change with sexual maturation leading to sexually dimorphic EOD with respect to waveform and/or duration (Hopkins 1980, 1981; Westby and Kirschbaum 1982; Bass and Hopkins 1985; Landsman 1993; Friedman and Hopkins 1996).

In our study, we address the first three of these four topics by examining the EO anatomy within the mormyrid genus *Campylomormyrus*. Among the 14 described species of this genus (Taverne 1972), there is an extraordinary diversity of EODs with respect to waveform and duration (Hopkins 1999; Feulner et al. 2008). Moreover, recent phylogenetic studies revealed that especially closely related species evolved strikingly different EODs (Feulner et al. 2008).

We examined the EODs and conducted histological examinations of the adult EO of *C. compressirostris*, *C. tamandua*, *C. tshokwe* and *C. numenius*. Our first goal was to investigate whether the observed differences in EOD are reflected in the anatomical organization of the EO.

Our second goal was to investigate how ontogenetic changes in the EOD correlate with ontogenetic changes in EO morphology. To shed light on this topic we have chosen the species *C. numenius*, for which we were able to document the development of both the EO and the EOD.

Materials and methods

The EOs of four *Campylomormyrus* species (see Table 1) were used for anatomical examinations via light

Table 1 Sampling of *Campylomormyrus* species for the histological investigations and the in situ dissections

Species	Gender/status	Total length (cm)	# of electrocytes
C. compressirostris ($n = 2$)	Female	14	–
	Female	14.5	75 ± 3
C. numenius ($n = 3$)	Juvenile	11.1	–
	Female	31	–
	Female	40	60 ± 3
C. tamandua ($n = 5$)	Female	24.6	–
	Female	7.5	87 ± 3
	Male	16.8	–
	Male	29.7	–
	Male	20	80 ± 3
C. tshokwe ($n = 4$)	Female	26.3	–
	Female	34	–
	Male	30.4	–
	Male	33.5	80 ± 3

Total length refers to the total body length of the fish

Number (#) of electrocytes is determined from one electrocyte column (the lower left seen from caudal)

This counting was achieved via in situ preparation and subsequent determination of the number of electrocytes via a binocular

microscopy and in situ dissection. For preparation of the histological slides, the fish were euthanized by an overdose of phenylethanol and the caudal peduncle was cut off. The part containing the adult EO was partitioned into a cranial and a caudal fraction. The tissue was fixed by immersion in Bouin's solution or in 4 % formalin, decalcified in the case of formalin fixation with 7.5 % EDTA (pH 7.4), dehydrated and embedded in paraffin following conventional techniques (Mulisch and Welsch 2010). The rostral part of the EO of each specimen was sectioned serially at 4–6 µm in the transverse plane, whereas the caudal portion was sectioned serially at 4–6 µm in the sagittal plane using a Leica 2035 Biocut microtome. Sections were mounted on glycerin/albumin-coated slides. Following deparaffinization and rehydration, sections were stained with Azan or HE (Mulisch and Welsch 2010), dehydrated and coverslipped with DePeX mounting medium (Sigma-Aldrich).

The sections were investigated with a Leica microscope DM4000B. Pictures were taken and processed by using the Leica DFC 480 camera together with the Leica IM software version 4.0. Morphometric measurements of electrocytes were taken with the tpsDig software version 2.17 (Rohlf 2013).

For the in situ dissection, skin was carefully removed from the part of the tail containing the EO and the number of electrocytes was determined either via macrophotography (Canon EOS 100D) or through inspection by eye.

Additionally, to analyze species-specific EOD characteristics, we used the EOD recordings from 82 animals caught in the wild during field trips to the Congo basin near Brazzaville in 2004, 2006 and 2012 (see Table 2). For EOD recordings in the field, the fish were held in a small plastic aquarium, 45 cm × 15 cm in size, filled with Congo stream water (conductivity: 40–70 µS/cm, temperature: 24–26 °C). The tank featured a compartment adjustable in size used to prevent the fish from freely swimming during the measurements. Stainless steel electrodes (V2A) were positioned at the rostral and caudal end of the fish with a distance of a few centimeters from the fish—the positive electrode was positioned next to the head. The EOD waveforms were displayed and recorded by a Tektronix TDS 3012B digital phosphor oscilloscope (sampling rate: 10 kHz; 9 bit vertical resolution) with a Tektronix ADA 400A differential preamplifier (variable gain from 0.1× up to 100×; bandwidth 100 Hz–1 MHz). The oscilloscope and preamplifier were AC coupled. The EOD data were transferred onto the hard drive of a computer via floppy disks. Per individual, one representative EOD was analyzed.

Five EOD characteristics were measured with a custom-made MATLAB script: the duration and relative amplitude of the two main phases (maximum and minimum), frequency as well as amplitude of the peak of the fast Fourier

Table 2 Sampling of *Campylomormyrus* species for the analyses of EOD characteristics

Species	Gender/status of specimens			Total number	Size range (cm)
	Juvenile	Male	Female		
C. compressirostris	3	19	9	31	10–29
C. numenius	23	1	2	26	11–44
C. tamandua	–	6	4	10	15–25
C. tshokwe	–	3	12	15	26–36

The total number refers to the specimens sampled and to the number of EODs (as one representative EOD per specimen was analyzed). The size range refers to the total body length of the fish. All specimens, except those of *C. tshokwe*, were analyzed histologically concerning gender and developmental state of the gonads

After EOD recording and subsequent fixation of the fish, the gonads were dissected and processed with conventional paraffin histological techniques (Mulisch and Welsch 2010)

Gonads containing spermatogonia or oocytes I (see Grier 1981; Wallace and Selman 1981 for terminology) indicated juvenile fish, whereas gonadal recrudescence (spermatocytes I and further spermatogenesis stages; oocytes I with yolk vesicle formation or vitellogenesis) indicated sexually mature fish. In addition, the presence of the sexual dimorphism of the anal fin (see Schugardt and Kirschbaum 2002) allowed the determination of the gender of the fish (for *C. tshokwe*)

Thus, we were able to determine the total length of juveniles and adult fish

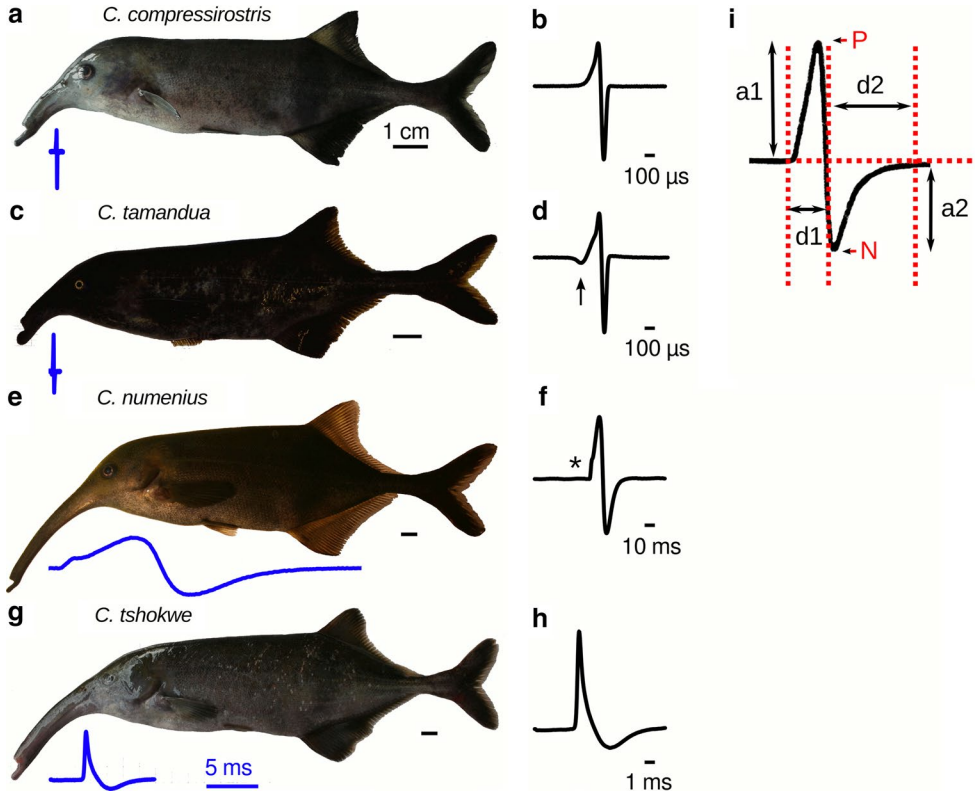

Fig. 1 Adults of four species of the genus *Campylomormyrus* (Taverne 1972) and their electric organ discharges (EODs). EODs below fish (in *blue*) are scaled to show the differences in duration among species. Note the different *scale bars* for the non-scaled EODs and the corresponding variation of EOD duration. **a**, **b** *C. compressirostris* possesses a brief biphasic EOD of less than 200 µs duration. **c**, **d** *C. tamandua* features a triphasic EOD of ~300 µs duration. The head-positive phase is preceded by a weak head-negative prepulse (*arrow*). **e**, **f** *C. numenius* exhibits a very long biphasic EOD of ~25 ms. The *asterisk* indicates an inflection point in the rising phase of the head-positive phase. **g**, **h** *C. tshokwe* possesses a biphasic EOD of ~4 ms duration. **i** *Dashed lines* indicate how characteristics of an EOD were measured exemplified by a biphasic EOD; *P* peak of the head-positive phase, *N* peak of the head-negative phase, *a* amplitude of P (a1) and *N* (a2), *d* duration of head-positive (d1)/head-negative phase (d2). *Scale bar* below fish is 1 cm in each case

transformation (FFT) and the number of phases including the optional pre- and post-phase (before or after the main positive and negative phase, not exhibited by all species). The first and last 2 % deviation from the peak-to-peak amplitude was taken as the starting and end point of each EOD.

Results

Characteristics of the adult electric organ discharge in *C. compressirostris*, *C. tamandua*, *C. tshokwe* and *C. numenius*

Figure 1 shows our four focus species of the genus *Campylomormyrus* and their adult EODs. The 82 examined EODs display no sexual dimorphism within any of the four species. However, potential seasonal dimorphisms have not been evaluated, as fish were only recorded once during the dry season. *C. compressirostris* exhibits a brief, biphasic EOD [average duration = 164.9 ± 15.49 (SD) µs, $n = 31$; see Fig. 1a]—the first phase of the EOD waveform is head positive followed by a second head-negative phase (Fig. 1b). The amplitudes of the head-positive peak (P; see Fig. 1i) and the head-negative peak (*N*) have an average ratio of 0.57 (SD = 0.039).

The EOD of *C. tamandua* is brief and basically triphasic (average duration = 315.9 ± 99.75 µs, $n = 10$; see Fig. 1c), i.e., it starts with a small head-negative pre-phase (Fig. 1d, arrow) followed by the main head-positive and head-negative phases. However, sometimes also a weak head-positive post-phase can be present (observed in 6 of the 10 analyzed individuals). The amplitude ratio of P/N is on average 0.59 (SD = 0.044).

In *C. numenius*, the EOD is biphasic and of very long duration (i.e., on average 25.4 ± 3.28 ms, $n = 3$; see Fig. 1e). The rising portion of the head-positive phase has a step-like inflection point (Fig. 1f, asterisk) and the *P*/*N* ratio is on average 1.23 (SD = 0.339).

C. tshokwe possesses a biphasic EOD (average duration = 3.7 ± 1.06 ms, $n = 15$; see Fig. 1g). Uniquely

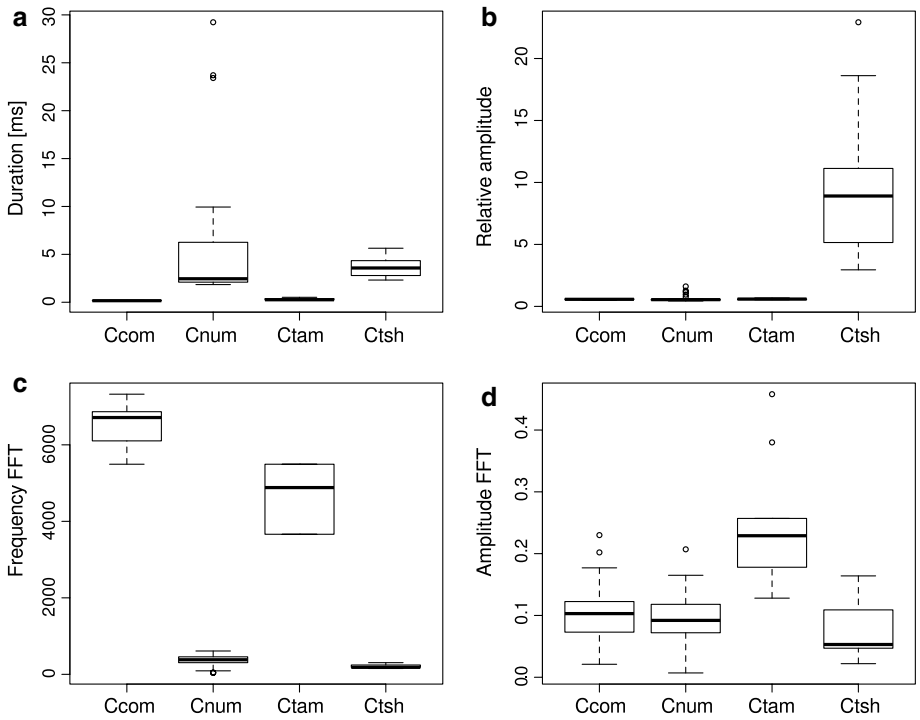

Fig. 2 Box plots revealing differences in electric organ discharge (EOD) characteristics across *C. compressirostris* (Ccom; $n = 31$), *C. numenius* (Cnum; $n = 26$), *C. tamandua* (Ctam; $n = 10$) and *C. tshokwe* (Ctsh; $n = 15$). The four characteristics shown are EOD duration (**a**), relative amplitude of main positive and negative phase (**b**), the frequency (**c**) and peak (**d**) of the fast Fourier transformation (FFT). Outlier values are indicated as *circles*

among the species analyzed here, the EOD of *C. tshokwe* rises steeply and is followed by a weaker and prolonged head-negative phase (on average more than twice as long as the head-positive phase; Fig. 1d). The *P*/*N* ratio is on average 9.49 (SD = 5.853).

Utilizing 82 EODs recorded in the wild, we additionally characterized species-specific differences across the four species (see Online Resource 1 for output of the MATLAB script). An analysis of four EOD characteristics demonstrated that EODs were significantly differentiated across the four species (MANOVA, Wilks, $p < 0.001$) (see also Fig. 2). No sex-specific differences between adults have been detected, while *C. numenius* showed significant differences between size groups with regard to EOD duration [juvenile 11 cm ($n = 8$), juvenile 12–22 cm ($n = 15$), females 33–44 cm ($n = 2$), males 32 cm ($n = 1$), ANOVA, $p < 0.001$]. Evaluating the different EOD characteristics by linear regressions revealed two correlations with total body length (a proxy for age), i.e., EOD duration in *C. numenius* (see Fig. 3a, b; $p < 0.001$) and relative amplitude of the two main peaks in *C. tshokwe* (see Fig. 3a, c; $p = 0.015$).

Anatomical characterization of the adult electric organ in *Campylomormyrus*

The four species of the genus *Campylomormyrus* possess an adult EO that conforms to the basic mormyrid bauplan as described, e.g., Marcusen (1864). As illustrated for *C. compressirostris* in Fig. 4, four columns of electrocytes surround the vertebral column between the posterior edge of the dorsal fin to the beginning of the caudal fin—a dorsal and a ventral column on each side. Each column contains a large population of regularly spaced, flat electrocytes (see Table 1 for details about absolute numbers) that are stacked behind each other and each column is enveloped in a connective tissue tube. Each electrocyte again is situated in a compartment that is confined by septa of connective tissue. In cross sections, the electrocyte's shape in the four species of *Campylomormyrus* ranges from almost round to kidney shaped and their absolute size varies according to the size of the fish. The diameter of the electrocytes is always about two orders of magnitude larger than the thickness, resulting in the typical disk-shaped appearance (Fig. 4d). Each electrocyte is characterized by distinguishable faces: the rostral membrane is referred to as the anterior face and the caudal membrane as the posterior face.

The evaginations of the electrocyte building the stalk system always originate on the posterior face in the four species. These stalks fuse repeatedly to become one major stalk. However, the branching pattern (number of fusions) and electrocyte geometry vary—in part considerably—among species (see the subsequent section).

In the following we describe the anatomical details of the electrocytes observed in sagittal and cross sections. The sagittal plane S1 (Fig. 4c) shows the electric organ in a lateral region, whereas the sagittal plane S2 shows a more medial aspect of the electric organ close to the spinal cord where the axon bundles of the electromotor neurons are in contact with the stalks.

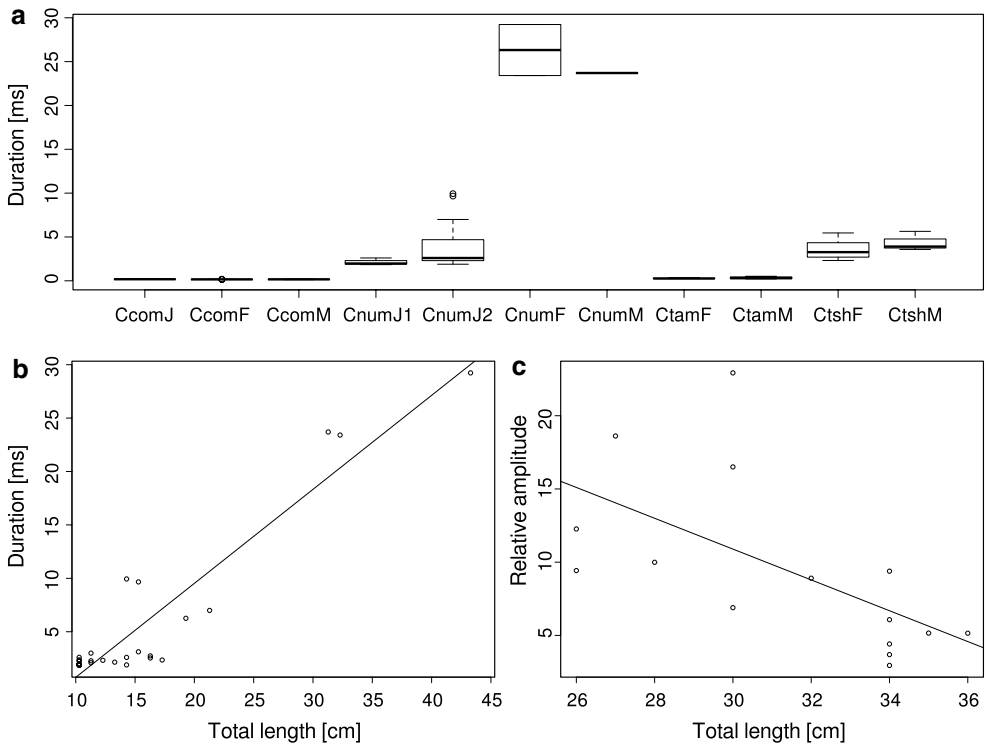

Fig. 3 Two of the analyzed *Campylomormyrus* species show correlation of a certain electric organ discharge (EOD) characteristic with total body length. **a** *Box plot* of EOD duration. Within the four species, juveniles, females and males are differentiated. Significant differences are only revealed between juveniles and adults of *C. numenius* [CnumJ1 juvenile 11 cm ($n = 8$), CnumJ2 juvenile 12–22 cm ($n = 15$), CnumF females 33–44 cm ($n = 2$), CnumM males 32 cm ($n = 1$), ANOVA, $p < 10^{-15}$]. No differences in EOD duration were detected in the other groups, i.e., among *C. compressirostris* [CcomJ juvenile 10–13 cm ($n = 3$), CcomF females 13–22 cm ($n = 9$), ComM males 13–29 cm ($n = 19$)], *C. tamandua* [CtamF females 16–22 cm ($n = 4$), CtamM males 15–25 cm ($n = 6$)] and *C. tshokwe* [CtshF females 26–35 cm ($n = 12$), CthsM males 34–36 cm ($n = 3$)]. **b** Linear regression of EOD duration and total length for *C. numenius*. The *line* indicates the fitted data ($R^2 = 0.874$, $p < 10^{-11}$). **c** Linear regression of relative amplitude of the two main phases of the EOD and total length for *C. tshokwe*. The *line* indicates the fitted data ($R^2 = 0.329$, $p = 0.015$). For the determination of the total length of juveniles and adults see legend of Table 2

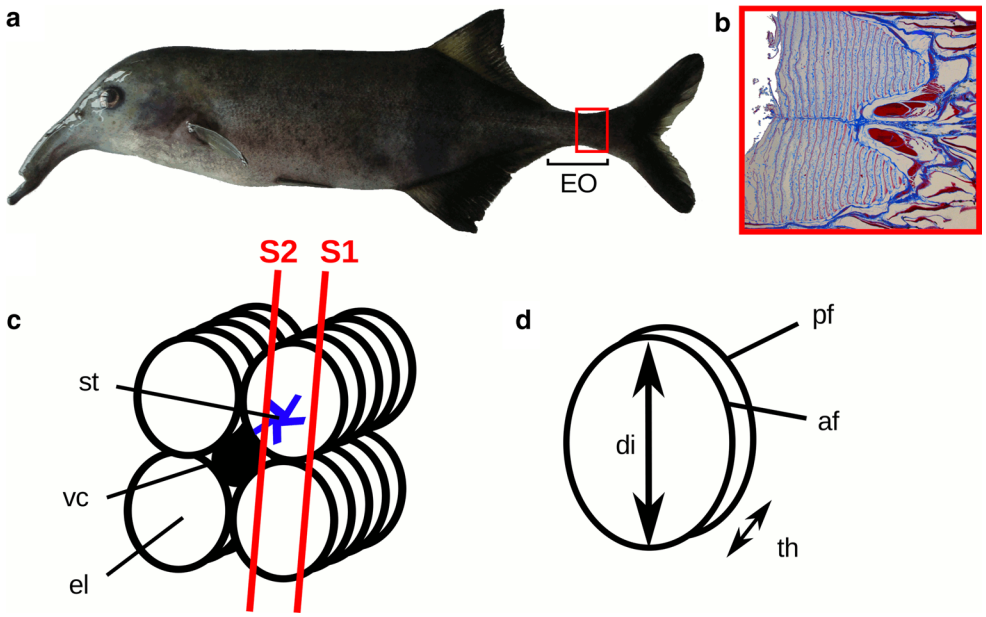

Fig. 4 Summary of location and organization of the electric organ (EO) in Mormyridae. **a** The location of the EO is shown by the example of *Campylomormyrus compressirostris*. **b** Histological sagittal section of the caudal part of the EO (see Fig. 4a, *red rectangle*). **c** Four columns of electrocytes (e) surround the vertebral column (vc) and one face of the cell possesses evaginations, which fuse to a stalk (st) and receive the innervation. *S1* sagittal plane at the periphery of the electrocytes (see Figs. 5, 6), *S2* sagittal plane close to the vertebral column (see Fig. 9). **d** Scheme of a *disk-shaped* electrocyte with its anterior (af) and posterior face (pf). Diameter (di) and thickness (th) of the electrocyte

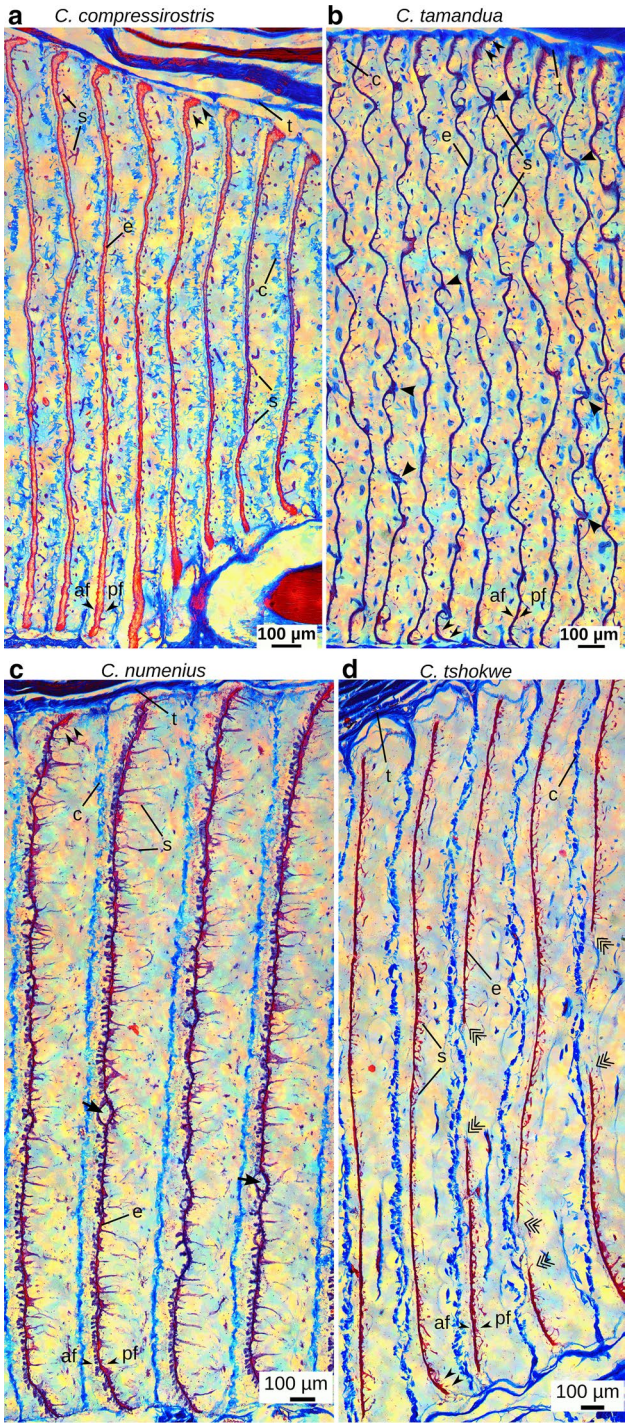

Fig. 5 Parasagittal sections from sectional plane S1 (see Fig. 4c) ▶ showing the general organization of the electrocytes (e) in four *Campylomormyrus* species. Azan stain. Rostral left, caudal right. The column of electrocytes is enveloped by a connective tissue tube (t); adjacent cells are separated and surrounded by connective tissue septa (c). Stalks (s) arise from the posterior face (pf) and the electrocytes bend caudad in their periphery making tight contact with the connective tissue (*double arrows*). **a** Electrocytes of *C. compressirostris.* Note that this photomicrograph is taken from the posterior edge of the electric organ; therefore, the diameter of cells decreases toward caudal. The electrocytes are comparatively thin at the center and increase in thickness toward the periphery. **b** Electrocytes of *C. tamandua*—the large arrowheads indicate stalks penetrating the cell body through holes in the cell body. The thin electrocytes undulate in their vertical plane giving a wave-like appearance. **a**, **b** The anterior face (af) of the electrocytes is smooth and exhibits no proliferations. **c** Electrocytes of *C. numenius.* The anterior face (af) of each electrocyte shows evaginations called papillae (p), which can merge and build cavities (*big arrows*) filled with extracellular matrix. **d** Electrocytes of *C. tshokwe* exhibit large pores (*tails*), where the cell's body is interrupted. The electrocytes are slightly thicker in their periphery than in the center and their anterior face is smooth

General organization of the electrocytes in *Campylomormyrus*

Campylomormyrus compressirostris

The EO of this species is built up of rather straight electrocytes running in parallel as seen in the parasagittal lateral section (Fig. 5a). The electrocyte's main body is relatively thin in its central region [6–11 µm, mean = 8.6 ± 1.8 (SD) µm, $n = 25$] and becomes thicker toward the dorsal and ventral periphery, where it measures on average 26.8 µm ($n = 25$, SD = 4.8). This increase in thickness is accompanied by a bending of the border area of the electrocytes, such that the surface area of the cell in this region is enlarged (Figs. 5a, 6a). This establishes a tight contact with the connective tissue, which surrounds each electrocyte.

The connective tissue septum constituting the boundary of each electrocyte's compartment is located closer to the anterior face than to the posterior face of the electrocyte (Figs. 5a, 6a). The space caudal to each electrocyte is filled with thin irregularly shaped stalks, which originate on the posterior face (Figs. 5a, 6a, b). These stalks soon fuse to become stalks of higher degree until they finally merge into one major stalk of large diameter. Except for the arising stalks, both faces of the electrocyte are smooth and exhibit no further proliferations or evaginations.

Campylomormyrus tamandua

In sagittal view the electrocytes have a wave-like appearance with sharp bends in regions where the small stalks penetrate the cell (Fig. 5b). The stalks originate on the posterior face of the electrocyte, but after merging to variable degree they turn anteriorly and penetrate the electrocyte (Fig. 6c, d). At the anterior face the stalks fuse to become stalks of higher degree (Fig. 6d) until they finally all merge into a major stalk of large diameter. The penetrations seem to be more numerous at the periphery of the electrocyte than in the center (Fig. 5b).

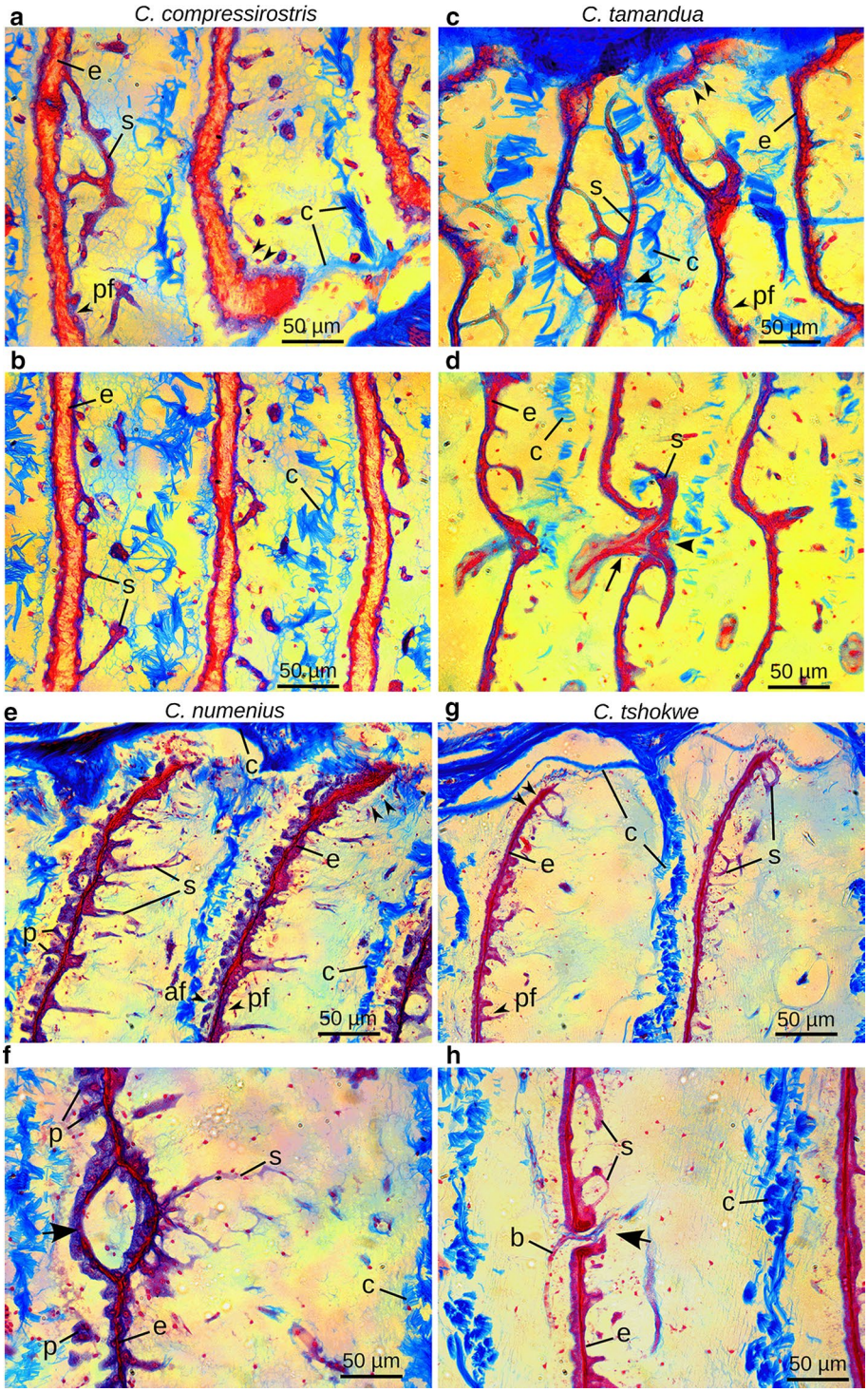

The electrocytes vary in thickness from 5 to 15 µm (mean = 8.6 ± 2.2 µm, $n = 25$). At the periphery, the electrocytes bend and run partially parallel to the surrounding connective tissue tube (Fig. 6c). The electrocytes are located in the center of the connective tissue compartments. The stalks originate on the posterior face of the electrocyte, while the major stalk is located anterior to the electrocyte.

Campylomormyrus numenius

This species exhibits straight electrocytes, with almost perfect parallel arrangement seen in the sagittal view (Fig. 5c). Numerous thin stalks arise at almost 90° angle from the posterior face of the cell. In contrast to *C. compressirostris* and *C. tamandua*, they fuse regularly, thereby forming a

◀**Fig. 6** Photomicrographs of Azan-stained sagittal section (sectional plane S1, see Fig. 4c, rostral left) of the electric organ (EO). Species names above the topmost pictures are valid for the respective picture column. **a**, **b** Sagittal sections of *Campylomormyrus compressirostris*' EO; **a** Small stalks (s) arise at the posterior face (pf) of the electrocyte (e) and fuse to become bigger stalks. At the periphery, the electrocyte bends caudad (*double arrowheads*) coming into tight contact with the connective tissue (c). **b** Central region of electrocytes showing the many small and irregularly shaped stalks originating posteriorly. Note that the electrocytes are thinner at the center than at the periphery (compare to **a**). **c**, **d** Sagittal sections of *C. tamandua*'s EO. **c** Small stalks arise at the posterior face of the electrocyte, fuse and penetrate the cell body (*large arrowhead*). At the periphery, the electrocytes bend (*double arrowheads*) making tight contact with the connective tissue enclosing each electrocyte. **d** Stalks turn anteriorly and penetrate the cell body (*arrowhead*). Anteriorly, the stalks fuse (*arrow*). In regions of penetrations, the electrocyte bends posteriorly. **e**, **f** Sagittal sections of C. *numenius*' EO. **e** The anterior face (af) of the electrocyte (e) exhibits numerous papillae (p) which tend to merge at the periphery where the electrocyte bends caudad and is in tight contact with the connective tissue (c) (*double arrowheads*). The stalks (s) arising at the posterior face (pf) are thin and numerous. **f** Papillae fuse and build a cavity (*big arrow*) accompanied by a caudad bending of the electrocyte. **g**, **h** Sagittal sections of *C. tshokwe*'s EO. **g** Many fine stalks arise at the posterior face and fuse. The thin electrocytes (e) bend at their periphery slightly caudad making tight contact with the connective tissue. **h** A small blood vessel (b) penetrates the electrocyte through a hole in its cell body (*big arrow*)

highly branched stalk system of alveolar-like appearance. A major stalk is not formed before the stalks reach the processes of the spinal nerve. The connective tissue around each electrocyte is located very close to the anterior face of the electrocyte, thus giving sufficient space for the long and straight stalks on the posterior face (Fig. 5c). A further characteristic feature of *C. numenius'* EO is the pronounced proliferation of the anterior surface of the electrocytes by numerous evaginations (we refer to them as papillae; see Fig. 6e, f). Especially in the peripheral region of the electrocyte, the papillae are closely packed and are even partially fused. The caudally directed bending of the electrocyte at the periphery (Fig. 6e) allows for tight contact with the surrounding connective tissue. Due to the presence of the papillae, the electrocytes achieve an average thickness of 41.6 µm ($n = 25$, SD = 10.8) with a maximum of up to 78 µm, while in regions lacking such papillae the cells are on average 11.6 µm thick ($n = 25$, SD = 4.5). Some papillae at the anterior face come into proximity to each other and finally merge to form a "cavity" filled with extracellular matrix (Figs. 6f, 7c). This association of papillae always co-occurs with the caudad curvature of the electrocyte. The proposed emergence of these cavities is depicted in Fig. 7 by different observed stages within one section. These structures apparently occur at random within the electrocyte (Fig. 5c).

Campylomormyrus tshokwe

The electrocytes are oriented almost parallel and their thickness slightly increases toward the periphery (Fig. 5d). At the periphery the electrocytes bend slightly caudad and they are in close contact with the connective tissue septum, which outlines each electrocyte compartment (Fig. 6g). Apart from these regions at the periphery, where the electrocyte can reach a thickness of 25 µm, the thickness ranges from 6 to 14 µm (mean = 10.1 ± 2.1, $n = 25$). The distance between the connective tissue septum and the

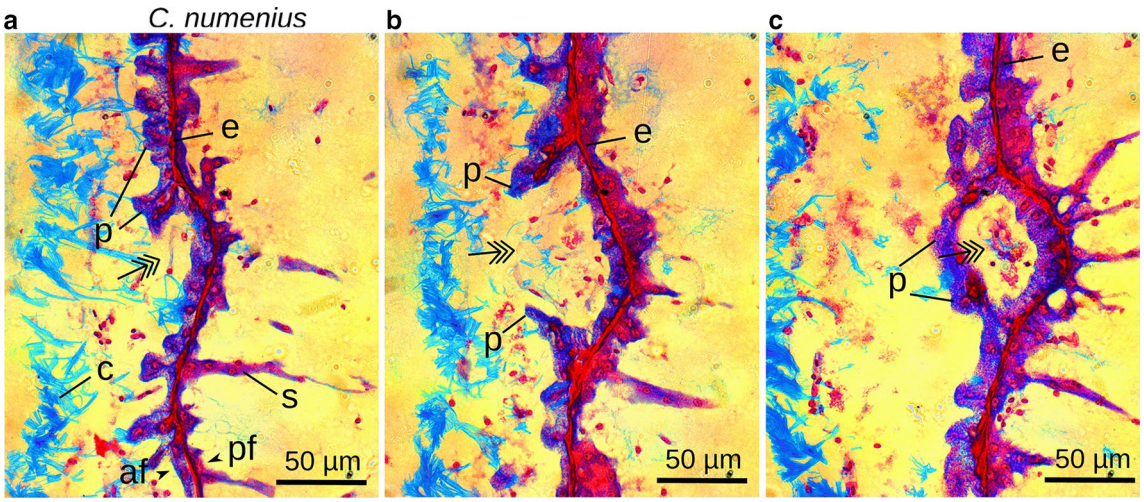

Fig. 7 Electrocytes (e) of *Campylomormyrus numenius* in sagittal view; Azan stain; rostral left. Stalks (s) arise at the posterior face (pf) and the anterior face (af) possesses papillae (p). The connective tissue (c) is close to the anterior face. The presumed formation of the cavities along the anterior face is shown for three different stages (**a**–**c**). **a** A fraction of the electrocyte starts to curve caudad (*tail*). **b** The curvature of the electrocyte is larger and the papillae of the anterior membrane start to converge (*tail*). **c** The papillae make contact to each other and enclose a compartment of extracellular space by forming a cavity (*tail*)

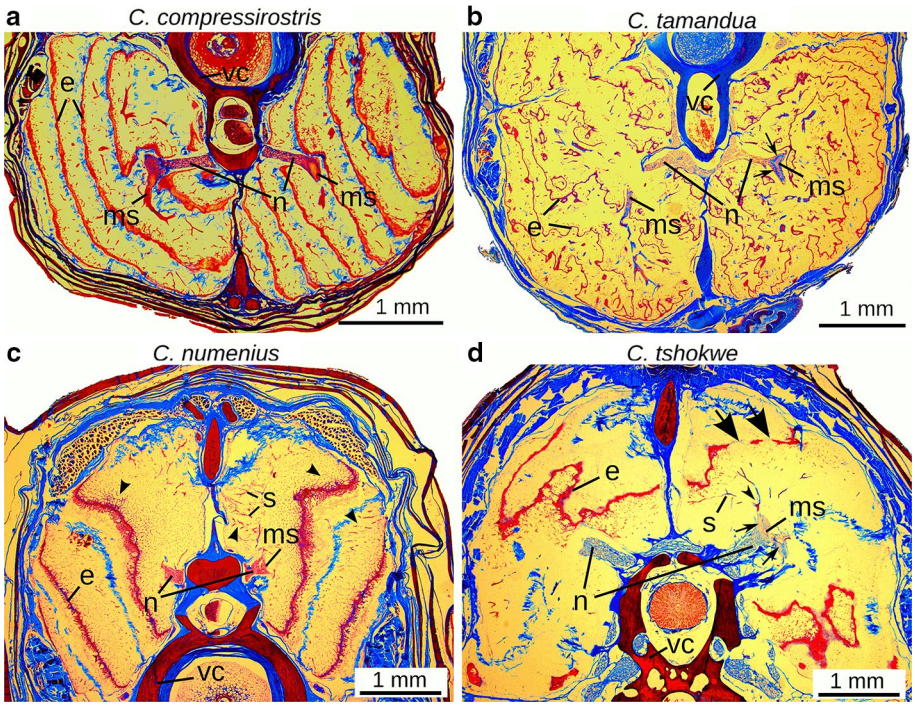

Fig. 8 Photomicrographs of Azan-stained cross sections of the electric organ (EO) for four *Campylomormyrus* species. **a**, **b** Electrocytes from the two ventral columns; see vertebral column (vc) for orientation of the EO. The processes of spinal nerves (*n*) extend deeply into the column of electrocytes in *C. compressirostris* and *C. tamandua*. The major stalk (ms) receives innervation in a restricted region. **b** The process of the spinal nerves bifurcates in dorsal and ventral directions (*arrows*). **c**, **d** Cross section of the EO. Electrocytes from the two dorsal columns; see vertebral column (vc) for orientation of the EO. **c** The stalk system is highly branched (*arrowheads*) and stalks are thin and ramified in *C. numenius*. The processes of the spinal nerve (*n*) remain close to the vertebral column and a major stalk (ms) is built only in the region of innervation. **d** Electrocytes exhibit large pores (*big arrows*) in *C. tshokwe*. The processes of the spinal neurons extend deeply into the columns of electrocytes and bifurcate in the dorsal and ventral directions (*arrows*). The dorsal fraction of the major stalk branches off early after receiving innervation from the spinal neurons in a restricted area (*small arrowhead*)

rostral face of the electrocyte comprises about 100 µm, and the distance to the caudal face amounts to about twice as much (Fig. 5d). The stalks originate at the posterior face of the electrocyte (Figs. 5d, 6g, h), remain on this side and finally merge to one major stalk. A distinctive feature of the electrocyte is the large pores or fenestrations in the cell body, which become particularly obvious in the sagittal view (Fig. 5d), but are also detectable in the cross section (Fig. 8d).

These interruptions in the electrocyte's body are not correlated in adjacent electrocytes and seem to appear at random. Furthermore, the electrocyte exhibits numerous small holes that are penetrated by blood vessels of various sizes (Fig. 6h).

Comparison of electrocyte organization among species

In *C. compressirostris*, *C. numenius* and *C. tshokwe*, the stalks emerge from the posterior face of the electrocyte and remain on this side, while merging to one major stalk. This electrocyte geometry is referred to as stalk of the NP_p type (Bass 1986).

C. tamandua deviates from this pattern [and can be described as the P_a type (Bass 1986): the stalks in this species also arise on the posterior face, but penetrate the cell body soon after their origin and fuse on the anterior side of the electrocyte to become one major stalk.

Among the four investigated *Campylomormyrus* species, there are important differences in the stalk system, i.e., in the degree of branching of stalks and the number of fusions of stalks before merging in a major stalk: in *C. compressirostris* and *C. tamandua,* the many small stalks merge soon after their origin into one major stalk of large diameter (Fig. 8a, b), while in *C. numenius* and *C. tshokwe* the stalk system is more branched, fusing into the major stalk just before reaching the electromotor nerve (Fig. 8c, d).

Campylomormyrus numenius features the following characteristic specializations: (1) the arrangement of stalks at their site of origin is very regular and most of the numerous stalks project in an almost 90° angle into the extracellular space (Fig. 5c). (2) In comparison with individuals of *C. tshokwe* of similar size, the electrocytes of *C. numenius* are remarkably thick due to the existence of pronounced papillae at the anterior face (compare Fig. 6e, g). (3) The

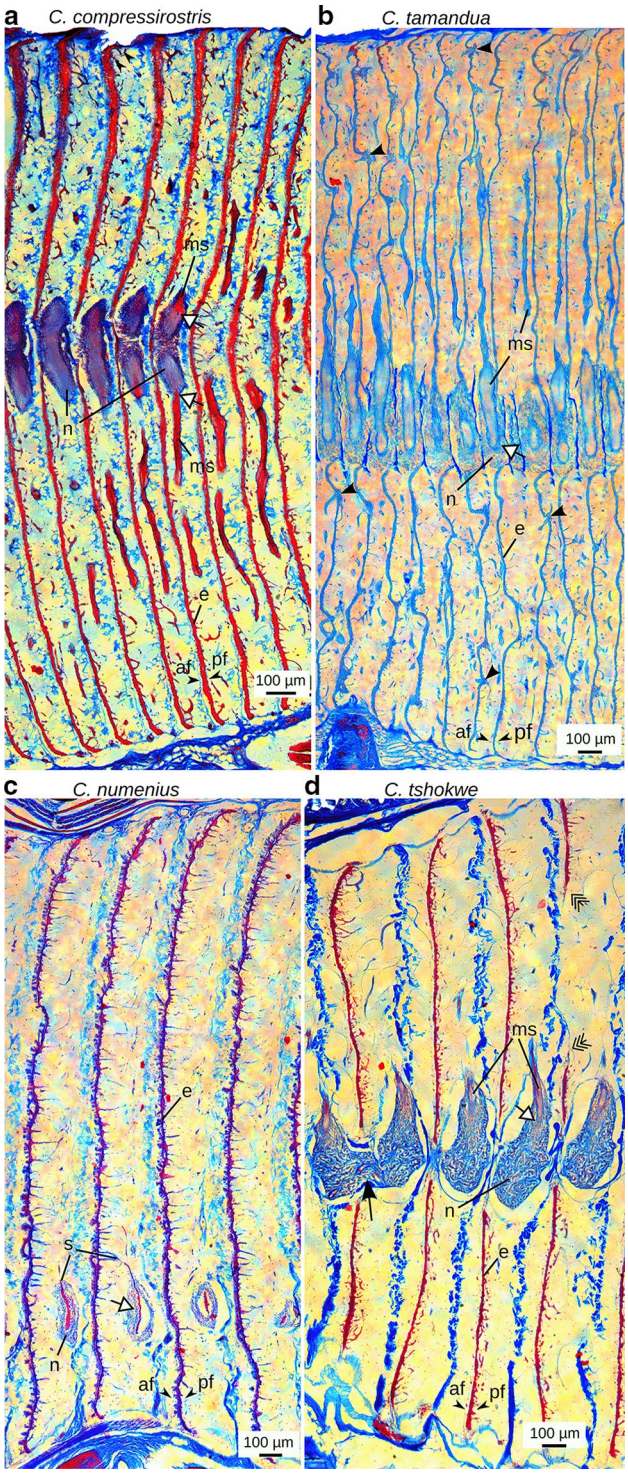

Fig. 9 Photomicrographs of Azan-stained parasagittal sections of several electrocytes (e) (sectional plane S2, see Fig. 4c; rostral left) for four *Campylomormyrus* species. **a**, **b** Processes of the spinal nerves (*n*) proceed up to the center of the column of electrocytes. Large major stalks (ms) make contact with the nerves of the electromotor neurons. **a** Innervated region of a dorsal and ventral process of the major stalk (*white arrows*) **b** Major stalks enclosed in axons of the nerve bundle processes (*white arrows*). Regions where thin stalks penetrate the electrocytes anteriorly are indicated by *arrowheads*. *af* anterior face, *pf* posterior face. **c** Processes of the spinal neurons (*n*) proceed in the space between electrocytes of *C. numenius* innervating small stalks (s), which fused after their origin at the posterior face (pf). **d** Massive spinal nerves pierce the electrocytes of *C. tshokwe* (*arrow*); their processes (n) proceed between the electrocytes. Major stalks are surrounded by axons of the spinal nerve processes (*white arrow*). One electrocyte is interrupted by large pores (region between *tails*). *af* anterior face

electrocyte's cell body is partially curved. Therefore, the papillae at the anterior face come in close proximity to one another and fuse at a later stage. Thereby, cavities filled with extracellular matrix are formed (Fig. 7).

A unique feature of *C. tshokwe* is the occurrence of large pores in the electrocyte's main body, which can encompass almost a quarter of the diameter of the electrocyte (see Fig. 5d). In *C. tshokwe* the electrocytes are often penetrated by blood vessels.

Comparison of innervation patterns of the electrocytes in the four species of *Campylomormyrus*

As shown by cross sections, the nerve fiber bundles of the electromotor neurons in *C. compressirostris*, *C. tamandua* and *C. tshokwe* extend deep into the column of electrocytes, whereas in *C. numenius* they remain close to their region of origin at the vertebral column (compare Fig. 8a–d).

In sagittal sections close to the midline, branches of the main nerve bundle, which run into the space between the electrocytes, can be seen in all four species (Fig. 9). Due to the above-described difference in the position of the main nerve, its branches are visible in medial aspects of the electrocyte columns of C. *compressirostris*, *C. tamandua* and *C. tshokwe,* but proceed closer to the vertebral column in *C. numenius*.

The nerve fiber bundles further branch within the space between electrocytes to envelope the stalks, which arrive from different peripheral directions. In the EO of *C. compressirostris, C. tamandua* and *C. tshokwe* the nerve bundle explicitly bifurcates in a dorsal and ventral branch (Figs. 8b, d, 9a). In accordance with this observation, a dorsal and ventral fraction of the stalk system fuses to become the major stalk. In *C. compressirostris* and *C. tamandua*, the stalks fuse to a major stalk before they reach the nerve (Figs. 9a, b, 10a, b), while in *C. tshokwe* numerous smaller stalks merge with the major stalk at the margin of the nerve (Figs. 8d, 10d).

In contrast, in *C. numenius* the nerve bundle can branch in more than two directions. This is in agreement with the highly ramified stalk system and the observation that more than two fractions of the stalk system travel toward the nerve. Sagittal sections of *C. numenius*' electrocytes reveal that already stalks of small diameter contact the nerve (Fig. 9c). Furthermore, a major stalk of larger diameter

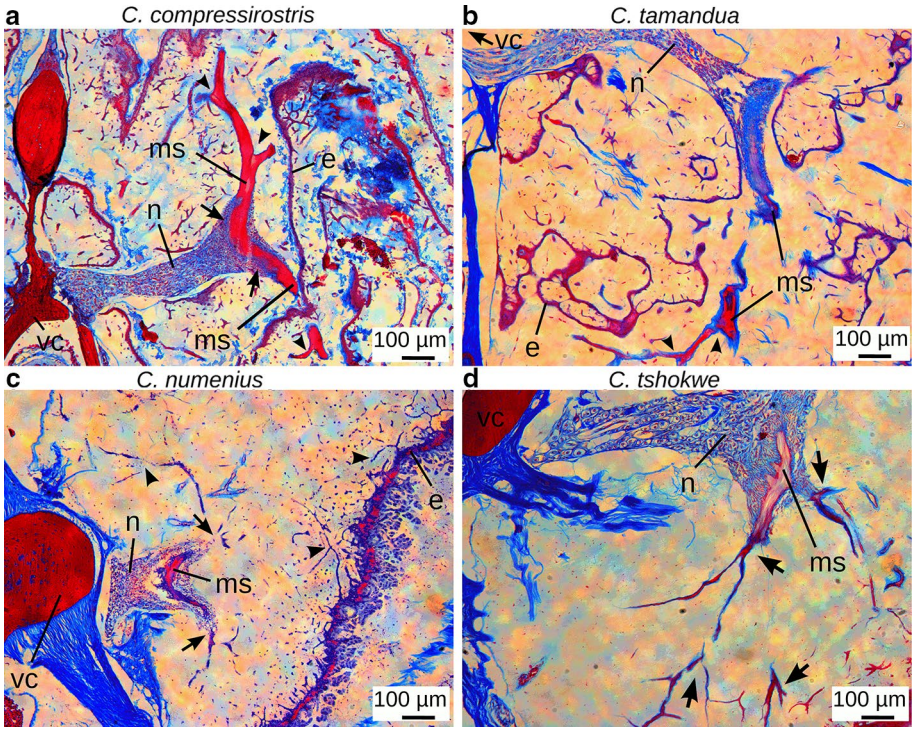

Fig. 10 Photomicrographs of Azan-stained cross sections from one column of the electric organ (EO) in four *Campylomormyrus* species; see the vertebral column (vc) for orientation of the EO. **a** Electrocyte (e) of a ventral column in *C. compressirostris*; a dorsal and ventral fraction of the massive major stalk (ms) meet and receive innervation from the bifurcated processes of the spinal nerves (n) (*arrows* indicate dorsal and ventral fraction of the nerve process). **b** Electrocyte of a ventral column in *C. tamandua*; a ventral branch of the major stalk makes contact with the spinal nerve process. **a**, **b** The major stalk furcates only rarely (*arrowheads*). **c** Electrocyte of a dorsal column in *C. numenius*; the major stalks at its site of innervation by spinal nerves. The major stalk branches multiple times at its site of innervation diminishing its diameter rapidly (*arrow*). The stalk system is dominated by fine stalks (*arrowheads*). **d** Electrocyte of a ventral column in *C. tshokwe*. A ventral branch of the major stalk enclosed in a process of the spinal nerve is shown, branching out multiple times after having received innervation (*arrows*)

can only be found within the mass of axons comprising the nerve (Fig. 10c).

Ontogeny of electric organ anatomy and electric organ discharge in *C. numenius*

We examined the EO of a juvenile, 11.1 cm-long specimen and an adult 31 cm-long specimen of *C. numenius* (Fig. 11a, d). These specimens show differences in overall morphology due to the positive allometric growth of the trunk-like snout. For the adult specimen, we were able to follow the dramatic change of the EOD waveform and duration during ontogeny for 3 years (Fig. 11b–d). As a juvenile, this individual featured an EOD with a duration of 3.4 ms, whereas as adult it produced an EOD of 28 ms duration (Fig. 11b, d). Throughout development, the EOD was biphasic, but the relationship of the duration for the head-positive and head-negative phase changed with age. In the juvenile, both phases of the biphasic EOD are of nearly equal duration (Fig. 11a), whereas the adult produces an EOD with the second head-negative phase being about three times longer in duration than the first head-positive phase (Fig. 11d). At intermediate age, the EOD is 12 ms in duration and the head-negative phase of the EOD is about two times longer in duration than the head-positive phase (Fig. 11c).

The basic electrocyte geometry (i.e., non-penetrating stalk system with posterior innervation, NP_P type) is of the same type, both in the juvenile and the adult fish, as is the compartmentalization of the EO (arrangement of the connective tissue septa surrounding the electrocyte) (Fig. 12). Furthermore, orientation and relative dimension of the innervating nerve fiber bundles are similar in the juvenile and adult EO. The nerve bundles stay close to the vertebral column and do not form a long branch extending deep into the space between electrocyte's faces.

Apart from these similarities, there are fundamental differences in the anatomy of the electrocytes between the two ontogenetic stages. Most striking are the prominent papillae of the anterior face of the adult fish's electrocyte, which are completely lacking in the juvenile specimen (Fig. 12a). Due to the lack of anterior papillae, the electrocytes in the juvenile are overall much thinner than in the adult, i.e., 6–12 µm

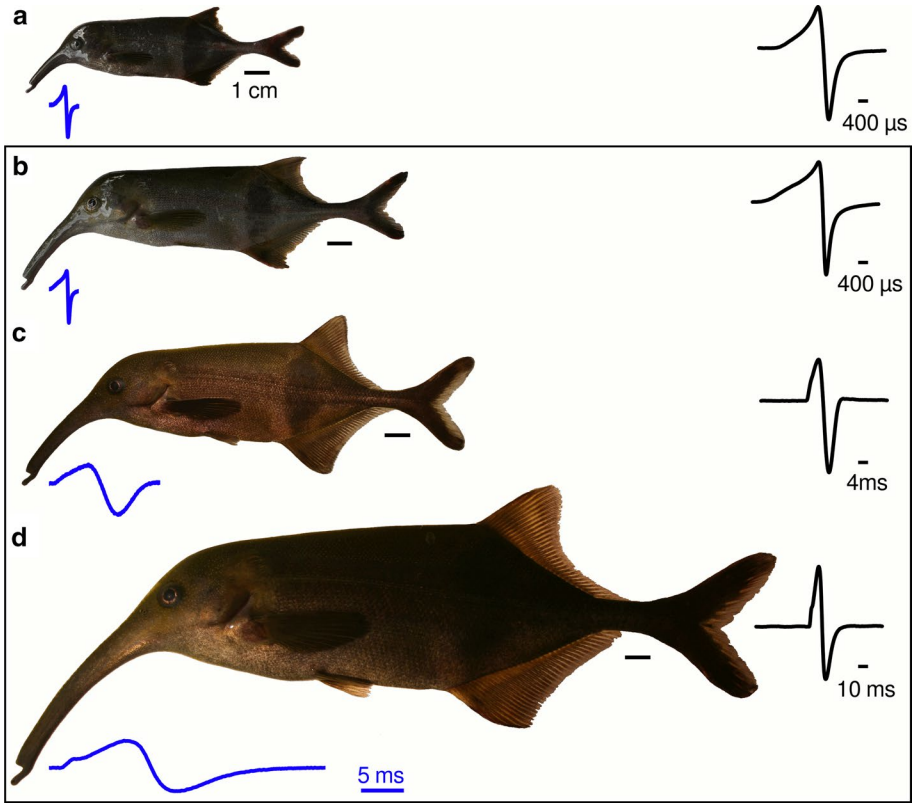

Fig. 11 Ontogeny of morphology and electric organ discharge (EOD) in *Campylomormyrus numenius*. Note the allometric growth of the trunk-like snout with increasing size of the fish (**a**–**d**). The EOD below the fish (in blue) is scaled to illustrate the increase in EOD duration. The change in EOD duration from the two juvenile specimens (**a**, **b**) to the adult specimen (**d**) is in the order of one magnitude. Further changes concern the relationship of the duration of the first and second pulse. To the right of each fish is the corresponding non-scaled EOD. **a** Individual caught in 2012; size = 11.1 cm. **b** Individual caught in 2006; size = 15.7 cm. Ontogeny of this specimen was followed for 3 years (see **c** and **d**). **c** The 2006-caught specimen recorded in 2007; size = 18.1 cm. **d** The 2006-caught specimen recorded in 2009; the individual reached sexual maturity; size = 31 cm. Note the differences in scale bars. *Scale bar* below fish is 1 cm in each case

(mean = 8.18, n = 25, SD = 1.49). Furthermore, the stalks arising on the posterior face are less numerous in the juvenile and the stalk system is less branched. After their origin on the posterior face, the stalks fuse more rapidly into stalks of higher degree and thus longer segments of major stalks are observed in the juvenile as compared to the adult (Fig. 13a, c).

After having received innervation, the major stalk remains longer of large diameter in the juvenile compared to the adult when extending into the periphery of the electrocyte (Fig. 13b, d).

Discussion

Correlation of electrocyte geometry/anatomy and electric organ discharge features among the four species of *Campylomormyrus*

The site of innervation is known to crucially determine the EOD waveform in mormyrids (Bennett and Grundfest 1961; Bennett 1971; Bass 1986): biphasic EODs usually correlate with stalks of the NP_p type, whereas triphasic EODs often occur in EOs with stalks of the P_a type. Our findings support previous data and modeling, since the only species with a triphasic EOD, *C. tamandua*, exhibits penetrating stalk electrocytes with anterior innervation. In contrast, the other three species analyzed here (*C. compressirostris*, *C. numenius* and *C. tshokwe*) possess non-penetrating stalk electrocytes with posterior innervation and discharge with biphasic waveforms. Our findings with regard to electrocyte geometry are also in accordance with observations from previous studies [*C. numenius* (Sullivan et al. 2000); *C. tamandua* (Bennett 1971; Sullivan et al. 2000); *C. compressirostris* (Bennett and Grundfest 1961)]. Our study is, however, the first one which directly compares electrocyte anatomy across species of the genus *Campylomormyrus*. It therefore provides first insights into some of the mechanisms enabling the enormous EOD variability among closely related species.

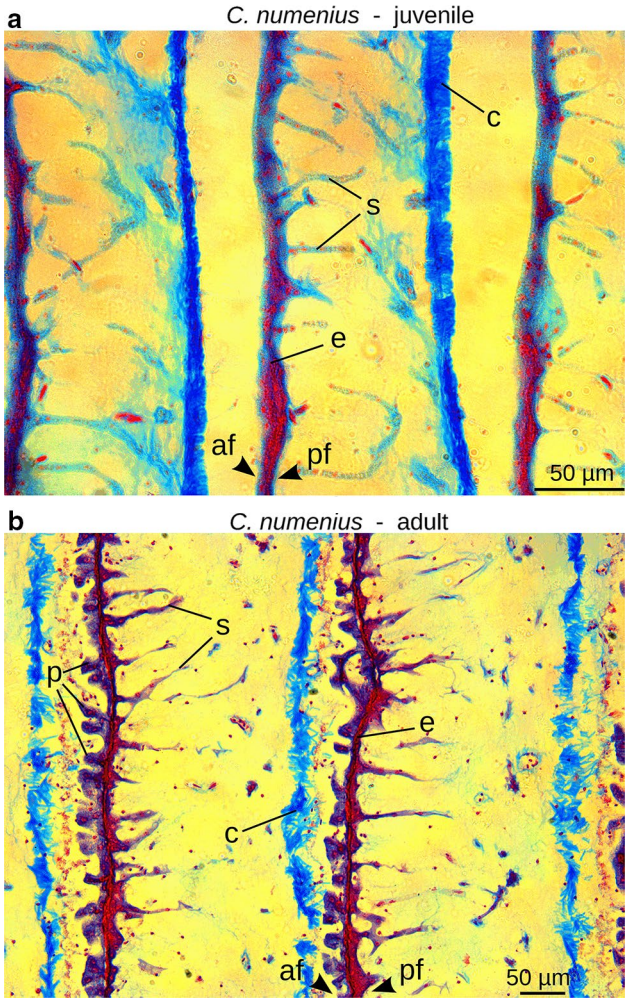

Fig. 12 Comparison of photomicrographs of parasagittal sections of the electric organ of a juvenile caught in 2012 (size = 11.1 cm) and the adult specimen of *Campylomormyrus numenius* caught in 2006 and recorded in 2009 (size = 31 cm). Azan stain; caudal right. Electrocyte geometry does not change during ontogeny; stalks arise in both specimens at the posterior face (pf) and proceed straight into the space between posterior face and the caudal connective tissue (c). **a** The anterior face (af) of the electrocyte (e) in the juvenile is smooth without surface proliferations. **b** The adult possesses numerous evaginations, called papillae (p), at the anterior face. Note difference in *scale bars*

Among the three investigated species with biphasic waveforms and basically identical electrocyte geometry, there are striking differences in EOD duration and appearance of the EOD waveform (see Fig. 1) that are accompanied by distinctive anatomical differences of the EO.

The biphasic EOD of very short duration in *C. compressirostris* correlates with the presence of smooth anterior and posterior electrocyte faces and the fact that these electrocytes possess a single major stalk of large diameter, which receives its innervation in one restricted area. This agrees with previous descriptions for several mormyrid species (Bass 1986), where a single focally innervated stalk seems to cause fast propagation of the action potential (AP) and fast depolarization of the posterior face contributing to the brief EOD. A fast activation of the anterior face can be expected from its smooth membrane surface lending a low capacitance to it, since the membrane capacitance is known as one important factor affecting the electrical excitability and the velocity of AP conduction (Carlson 2002).

The electrocytes of *C. numenius* differ from those of *C. compressirostris* with regard to the structure of the anterior face and the appearance of the stalk system. The long EOD duration probably depends on two morphological aspects: (1) the anterior face of electrocytes exhibits a pronounced surface proliferation due to papillae. This feature is expected to significantly increase the membrane capacitance of the electrocytes, thereby prolonging the membrane's time constant, i.e., the velocity at which the AP is propagated along the electrocyte's membrane will be decreased. Bass et al. (1986) have already reported on a direct correlation between increasing membrane surface area and increasing EOD duration. (2) In *C. numenius* there is a highly branched network of stalks, i.e., the stalks are of small diameter even close to their region of innervation (i.e., no major stalk of large diameter is yet formed). Accordingly, the surface area of the electrocyte becomes enlarged by the presence of numerous stalks of small diameter compared, e.g., to a species with a large and sparsely ramified stalk like *C. compressirostris* or *C. tamandua*. Therefore, the capacitance of the stalk membrane is larger. This feature—together with the small diameter of the stalks—may cause a decrease in the propagation velocity of the APs within these branches. This might explain the long activation time of the posterior face and the accordingly long duration of the head-positive pulse.

C. tshokwe features an EOD of intermediate duration compared to *C. compressirostris* and *C. numenius*. Its electrocytes are similar to those of *C. compressirostris* with smooth anterior and posterior faces and a non-penetrating large stalk. However, compared to *C. compressirostris,* more stalks arise at the posterior face, the stalk system is more intensively branched and the major stalk bifurcates multiple times after having received innervation. Therefore, an elongated head-positive pulse could be expected due to an increased requirement of time for AP propagation along the stalks to the posterior face. Yet, in comparison to the EOD of *C. numenius*, the head-positive phase is shorter in *C. tshokwe* and its rising phase is very steep. There is no morphological correlate associated with this steep slope, but it is imaginable that a heterogeneous ion channel repertoire (e.g., channels with fast kinetics in the posterior face's membrane) might be responsible for this EOD characteristic (Bennett 1970; Caputi et al. 2005). To test this hypothesis is beyond the scope of these

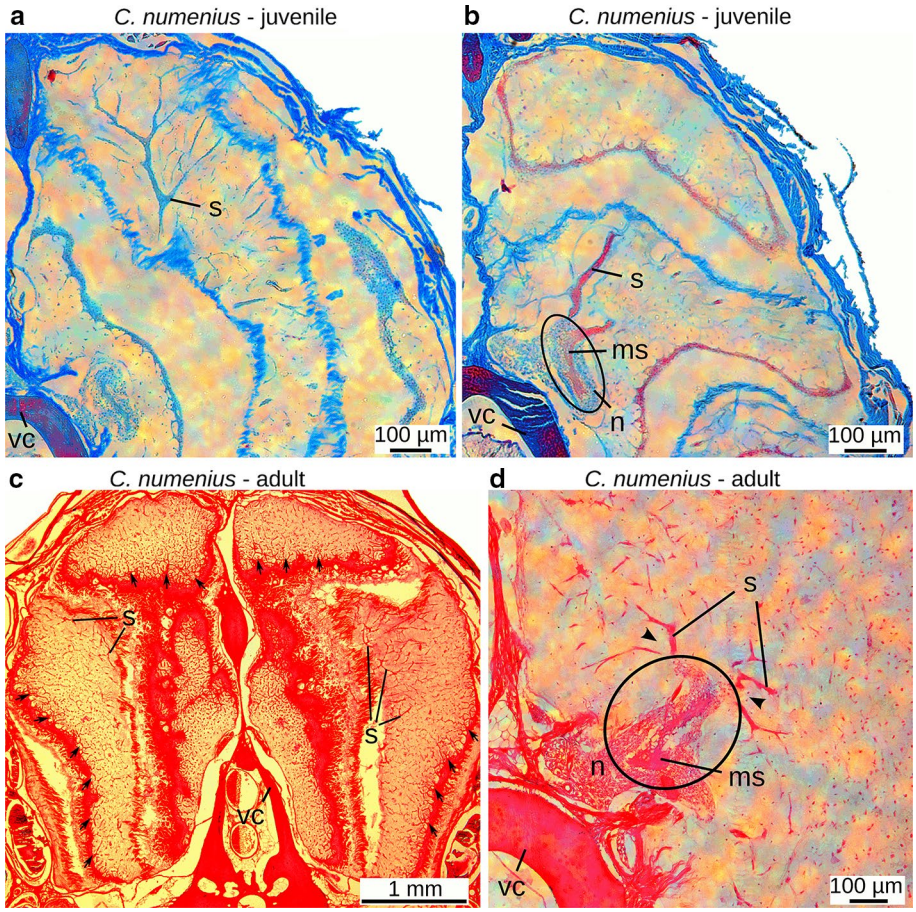

Fig. 13 Photomicrographs of cross sections from one column of the electric organ (EO) for two ontogenetic stages of *Campylomormyrus numenius*—the juvenile (see **a** and **b**) was 11.1 cm long and the adult (see **c** and **d**) measured 31 cm. See the vertebral column (vc) for orientation of the EO. **a** The stalk (s) in the juvenile is less branched than in the adult (compare to **c**); Azan stain. **b**, **d** Spinal motor neurons (n) extend into the electrocyte column and innervate the major stalk (ms) of an electrocyte (region in *circle*). **b** The major stalk bifurcates more sparsely in the juvenile and remains longer of big diameter (compare to **d**); Azan stain. **c** The stalk in the adult is highly branched; especially at the periphery of the electrocyte the stalk branches like a network (*small arrows*); HE stain. **d** The major stalk furcates already within the mass of axons comprising the nerve process and several stalks of smaller diameter branch off after leaving the nerve bundle (*arrowheads*); HE stain

histological examinations, as this would call for comparative studies on ion channel abundance and distribution across the distinct faces and the stalk among the different investigated species.

Whether the large fenestrations (pores) in the electrocyte's cell body of *C. tshokwe* have an influence on EOD waveform/duration or, more specific, the small amplitude of the head-negative pulse, remains to be examined. It is reasonable to assume that these fenestrations allow for the flux of, e.g., sodium ions from the extracellular space of one face to the other face. The summed flow of this positive charge along the body axis by leak current could diminish the net flow of positive charge, which is initially caused by activation of the anterior or posterior face, respectively.

Since the relative amplitude of the EOD's two main phases changes with total body length in *C. tshokwe*, we checked for a relationship between the degree and size of these fenestrations and total body length of the fish, but this analysis did not reveal any correlation.

C. tamandua exhibits an electrocyte geometry of the P_a type. The triphasic nature of its EOD is in full agreement with the prediction for this electrocyte anatomy (Bennett and Grundfest 1961; Bennett 1971). As a result of tunneled current flow along the stalks, which penetrate the electrocytes, a net flow of current runs from anterior to posterior and produces the small head-negative pre-phase of the EOD. Subsequent activation of the posterior face causes current flow in the posterior–anterior direction and hence a head-positive phase is measurable externally. Caused by the depolarization of the posterior face, also the anterior face becomes active and fires an AP. As result, the current flow is reversed and a final head-negative phase will be generated. Further, smooth anterior and posterior faces and a large, sparsely ramified stalk contribute to the overall brief EOD in this species.

Membranes of single electrocytes appear wavy in *C. tamandua*, the only species in this study with penetrating stalks. We cannot exclude that this is an artifact due to tissue shrinking during fixation. However, this wavy appearance was detected in all three *C. tamandua* specimens examined and absent in any specimen of the other three species with non-penetrating stalk. Interestingly, the same wavy appearance is also visible in other mormyrids with penetrating stalks such as *Paramormyrops kingsleyae* or *Brienomyrus brachyistius* (Gallant et al. 2011, 2012).

Ontogenetic change of electrocyte's anatomy and electric organ discharge in *C. numenius*

As discussed above, the EOD waveform and duration in the adult *C. numenius* can be partially explained by the anatomy of the EO, in particular by the characteristics of the anterior membrane of the electrocyte and the branching pattern of the stalk system. The much shorter EOD of the juvenile is based on a clearly different anatomy: (1) papillae on the anterior face of the electrocyte are completely missing in the juvenile's EO; (2) the stalk system is less branched than in the adult. A less branched stalk system should propagate the excitation faster and with less temporal delay to the posterior face leading to a more prompt activation of the caudal face by the stalk potential and thus a shorter head-positive phase. Further, the lack of papillae causes a much lower membrane capacitance of the anterior face in juvenile *C. numenius* compared to adults, which will boost the membrane's electrical excitability. This feature hence accounts for immediate response to depolarization and the subsequent short AP fired by this face.

The shift in EOD duration in the larger, but still juvenile, specimen of *C. numenius* (Fig. 9c) suggests a beginning increase of surface proliferation by the emergence of papillae on the anterior face. Such changes in membrane properties are known to be induced by gonadal steroid hormones (Bass et al. 1986). Therefore, the ontogenetic development of the EOD might be accompanied by changing plasma levels of steroid hormones. Whether the same hormone triggers these anatomical changes in both males and females of *C. numenius* or if other developmental processes are responsible has to be revealed by future investigations.

The understanding of the ontogenetic processes concerning the EO and the EOD is partially compromised by some authors having erroneously considered juveniles as a separate species—based on their deviant EOD (e.g., *C.* sp. B studied by Hopkins 1999; Trzcinski and Hopkins 2008—according to our study of the EOD ontogeny—a juvenile stage of *C. numenius*). Further, we do not know how the EOD of even younger and thus smaller juveniles of *C. numenius* (<11 cm) look like, i.e., whether the observed positive correlation between total body length and EOD duration persists or if there is a size range in which the EOD duration is constant. Therefore, we cannot estimate how many mechanisms (beyond proliferation of the anterior face and increasing furcation of the stalk system) are being involved in EOD development in this mormyrid species.

For future investigations, it would be interesting to study the ontogenetic EOD change in additional species, as there is at least one more species, respectively, species complex within the genus *Campylomormyrus* (i.e., *C. alces*) for which ontogenetic change in EOD duration has been observed (Trzcinski and Hopkins 2008; unpublished results).

Conclusion and outlook

Three of the examined species exhibit rather different EOD waveforms, despite similar electrocyte geometry. Here, the distribution and repertoire of ion channels could play a role in generating these inter-species differences (Caputi et al. 2005). A study on a representative of Gymnotiformes revealed that voltage-dependent ion channel kinetics correlate with AP duration and membrane excitability (McAnelly and Zakon 2000). Furthermore, in a gymnotiform fish, sex-specific EOD differences were related to expression levels of genes encoding voltage-gated potassium channel subunits (Few and Zakon 2007). Therefore, studies on the expression levels of genes encoding for voltage-gated sodium and potassium channels within the EO as well as on the distribution of these ion channels across the electrocyte would be highly welcome. One member of voltage-gated sodium channels is a particularly promising candidate for subsequent studies on ion channel distribution and abundance, since the expression of this member is known to be restricted to the EO in several electric fish species (Zakon et al. 2006).

So far, we have not discovered any sexual dimorphism within the EODs of the examined *Campylomormyrus* species. However, each individual was only recorded once during sampling in the dry season. Therefore, it is possible that seasonal changes occurred, which we did not capture. Particularly large males might possess deviant EODs, but those were underrepresented in our data set, as those are rare. To further examine sexual dimorphism in EOD, further sampling of large individuals during the spawning season (wet season) would be required.

The ontogenetic changes in the EO of *C. numenius* at the histological level were investigated with light microscopic techniques. Here, EM studies could unravel further details of membrane changes during ontogeny.

The elongated EOD is a derived character, shared by *C. numenius* and its sister species *C. rhynchophorus* (Feulner et al. 2008; unpublished results). It would be hence very interesting to study the EOD ontogeny and fine structure of the electrocytes in *C. rhychophorus* as well.

Acknowledgments We thank S. Abelt, H. Höft and D. Bernau for technical assistance. Financial support is acknowledged from the University of Potsdam and the Leibniz-SAW project GENART. Further, financial support is acknowledged from Deutsche Forschungsgemeinschaft (TI 349/1-1 and TI 349/1-2).

Ethical approval All applicable international, national and/or institutional guidelines for the care and use of animals were followed.

References

Alves-Gomes JA, Hopkins CD (1997) Molecular insights into the phylogeny of Mormyriform fishes and the evolution of their electric organs. Brain Behav Evol 49:324–350. doi:10.1159/000113223

Bass AH (1986) Species differences in electric organs of mormyrids: substrates for species-typical electric organ discharge waveforms. J Comp Neurol 244:313–330. doi:10.1002/cne.902440305

Bass AH, Hopkins C (1985) Hormonal control of sex differences in the electric organ discharge (EOD) of mormyrid fishes. J Comp Physiol A 156:587–604. doi:10.1007/BF00619109

Bass AH, Denizot JP, Marchaterre MA (1986) Ultrastructural features and hormone-dependent sex differences of mormyrid electric organs. J Comp Neurol 254:511–528. doi:10.1002/cne.902540405

Bell CC, Bradbury J, Russell CJ (1976) The electric organ of a mormyrid as a current and voltage source. J Comp Physiol 110:65–88. doi:10.1007/BF00656782

Bell CC, Libouban S, Szabo T (1983) Pathways of the electric organ discharge command and its corollary discharges in mormyrid fish. J Comp Neurol 216:327–338. doi:10.1002/cne.902160309

Bennett MVL (1970) Comparative physiology: electric organs. Ann Rev Physiol 32:471–528. doi:10.1146/annurev.ph.32.030170.002351

Bennett MVL (1971) Electric organs. In: Hoar WS, Randall DJ (eds) Fish physiology vol. V—sensory systems and electric organs. Academic Press, New York, London, pp 347–491. doi:10.1016/S1546-5098(08)60051-5

Bennett MVL, Grundfest H (1961) Studies on the morphology and electrophysiology of electric organs. III. Electrophysiology of electric organs in mormyrids. In: Chagas C, Paes de Carvalho A (eds) Bioelectrogenesis. Elsevier, London, New York, pp 113-135

Bruns V (1971) Elektrisches organ von *Gnathonemus* (Mormyridae) Elektrische Platte und Innervation. Zeitung für Zellforsch 122:538–563. doi:10.1007/BF00936087

Caputi AA, Carlson BA, Macadar O (2005) Electric organs and their control. In: Bullock TH, Hopkins CD, Popper AN, Fay RR (eds) Electroreception. Springer, New York, pp 420–424. doi:10.1007/0-387-28275-0_14

Carlson BA (2002) Electric signaling behavior and the mechanisms of electric organ discharge production in mormyrid fish. J Physiol Paris 96:405–419. doi:10.1016/S0928-4257(03)00019-6

Cheng C (2012) Morphological correlates of signal variation in weakly electric mormyrid fish. Honors Thesis, Cornell University

Denizot JP, Kirschbaum F, Westby GWM, Tsuji S (1982) On the development of the adult electric organ in the mormyrid fish *Pollimyrus isidori* (with special focus on the innervation). J Neurocyt 11:913–934. doi:10.1007/BF01148308

Feulner PGD, Kirschbaum F, Tiedemann R (2008) Adaptive radiation in the Congo River: an ecological speciation scenario for African weakly electric fish (Teleostei; Mormyridae; *Campylomormyrus*). J Physiol 102:340–346. doi:10.1016/j.jphysparis.2008.10.002

Few W, Zakon H (2007) Sex differences in and hormonal regulation of Kv1 potassium channel gene expression in the electric organ: molecular control of a social signal. Dev Neurobiol 67:535–549. doi:10.1002/dneu.20305

Freedman EG, Olyarchuk J, Marchaterre MA, Bass AH (1989) A temporal analysis of testosterone-induced changes in electric organs and electric organ discharges of mormyrid fishes. J Neurobiol 20:619–634. doi:10.1002/neu.480200703

Friedman MA, Hopkins CD (1996) Tracking individual mormyrid electric fish in the field using electric organ discharge waveforms. Anim Behav 51:391–407. doi:10.1006/anbe.1996.0037

Gallant JR, Arnegard ME, Sullivan JP et al (2011) Signal variation and its morphological correlates in *Paramormyrops kingsleyae* provide insight into the evolution of electrogenic signal diversity in mormyrid electric fish. J Comp Physiol A 197:799–817. doi:10.1007/s00359-011-0643-8

Gallant JR, Hopkins CD, Deitcher DL (2012) Differential expression of genes and proteins between electric organ and skeletal muscle in the mormyrid electric fish Brienomyrus brachyistius. J Exp Biol 215:2479–2494. doi:10.1242/jeb.063222

Grant K, Bell CC, Clausse S, Ravaille M (1986) Morphology and physiology of the brainstem nuclei controlling the electric organ discharge in mormyrid fish. J Comp Neurol 245:514–530. doi:10.1002/cne.902450407

Grier JH (1981) Cellular organization of the testis and spermatogenesis in fishes. Am Zool 21:345–357. doi:10.1093/icb/21.2.345

Hopkins CD (1980) Evolution of electric communication channels of mormyrids. Behav Ecol Sociobiol 7:1–13. doi:10.1007/BF00302513

Hopkins CD (1981) On the diversity of electric signals in a community of mormyrid electric fish in West Africa. Am Zool 21:211–222. doi:10.1093/icb/21.1.211

Hopkins CD (1999) Design features for electric communication. J Exp Biol 202:1217–1228

Hopkins CD, Bass AH (1981) Temporal coding of species recognition signals in an electric fish. Science 212:85–87. doi:10.1126/science.7209524

Kirschbaum F (1977) Electric-organ ontogeny—distinct larval organ precedes adult organ in weakly electric fish. Naturwissenschaften 64:387–388. doi:10.1007/BF00368748

Kirschbaum F (1982) Die Entwicklung des "adulten" elektrischen Organes bei *Pollimyrus isidori* (Mormyridae, Teleostei). Verh Dtsch Zool Ges 75:242

Kramer B (1996) Electroreception and communication in fishes. Gustav Fischer, Stuttgart, pp 44–73

Kramer B, Kuhn B (1994) Species recognition by the sequence of discharge intervals in weakly electric fishes of the genus *Campylomormyrus* (Mormyridae, Teleostei). Anim Behav 48:435–445. doi:10.1006/anbe.1994.1257

Landsman RE (1993) Sex-differences in external morphology and electric organ discharges in imported *Gnathonemus petersii* (Mormyriformes). Anim Behav 46:417–429. doi:10.1006/anbe.1993.1211

Lissmann HW (1958) On the function and evolution of electric organs in fish. J Exp Biol 35:156–191

Marcusen J (1864) Die Familie der Mormyren. Eine anatomisch-zoologische Abhandlung. Eggers et Comp, St Petersburg, pp 89–104

McAnelly ML, Zakon HH (2000) Coregulation of voltage-dependent kinetics of Na^+ and K^+ currents in electric organ. J Neurosci 20:3408–3414

Moller P (1970) "Communication" in weakly electric fish, *Gnathonemus niger* (Mormyridae) I. Variation of electric organ discharge (EOD) frequency elicited by controlled electric stimuli. Anim Behav 18:768–786. doi:10.1016/0003-3472(70)90026-6

Mulisch M, Welsch U (2010) Romeis-Mikroskopische Technik, 18th edn. Spektrum, Heidelberg

Ogneff J (1898) Einige Bemerkungen über den Bau des schwachen elektrischen Organs bei den Mormyriden. Zeitschrift für wissenschaftliche Zool 64:565–595

Rohlf FJ (2013) TpsDig, Version 2.17, Department of Ecology and Evolution, State University of New York at Stony Brook. Stony Brook

Rüppel E (1832) Fortsetzung der Beschreibung und Abbildung mehrerer neuen Fische im Nil entdeckt. Frankfurt a.M

Schlichter H (1906) Über den feineren Bau des schwach elektrischen Organs von *Mormyrus oxyrhinchus*. Zeitschrift für wissenschaftliche Zool 84:479–525

Schugardt C, Kirschbaum F (2002) Nilhechte des "Formenkreises" *Campylomormyrus numenius*: Bemerkungen zur Ontogenese des

Habitus, der elektrischen Entladung sowie zum Fortpflanzungsverhalten. In: Greven H, Riehl R (eds) Verhalten von Aquarienfischen II. Birgit Schmettkamp Verlag, Bornheim, pp 137–146

Schwartz IR, Pappas GD, Bennett MV (1975) The fine structure of electrocytes in weakly electric teleosts. J Neurocytol 4:87–114. doi:10.1007/BF01099098

Sullivan JP, Lavoué S, Hopkins CD (2000) Molecular systematics of the African electric fishes (Mormyroidea: Teleostei) and a model for the evolution of their electric organs. J Exp Biol 203:665–683

Szabo T (1956) Sur la structure et le type d'innervation de l'électroplaque d'un Mormyre. C R Acad Sci 242:2045–2048

Szabo T (1957) Le muscle d'origine de l'organe electrique d'un Mormyre. Zeitschrift für Zellforsch und Mikroskopische Anat 47:77–79. doi:10.1007/BF00340005

Szabo T (1958) Structure intime de l'organe electrique de trois Mormyrides. Zeitschrift für Zellforsch 40:33–45. doi:10.1007/BF00335061

Szabo T (1960) Development of the electric organ of Mormyridae. Nature 188:760–762. doi:10.1038/188760b0

Szabo T (1961) Rapports onto génétique s entre l'organe électrique, son innervation et sa commande encéphalique (*Mormyrus rume*). Zeitschrift für Zellforsch und Mikroskopische Anat 55:200–203. doi:10.1007/BF00340930

Taverne L (1972) Ostéologie des genres *Mormyrus* Linné, *Mormyrops* Müller, *Hyperopisus* Gill, *Isichthys* Gill, *Myomyrus* Boulenger, *Stomatorhinus* Boulenger et *Gymnarchus* Cuvier considérations générales sur la systématique des poissons de l`ordre des Mormyriformes. MRAC, Tervuren

Trzcinski N, Hopkins CD (2008) Electric signaling and electroreception properties in electric fishes of the genus, *Campylomormyrus* Mormyridae. Cornell Synap 2:19–22

Von der Emde G (1999) Active electrolocation of objects in weakly electric fish. J Exp Biol 202:1205–1215

Von Der Emde G (2006) Non-visual environmental imaging and object detection through active electrolocation in weakly electric fish. J Comp Physiol A 192:601–612. doi:10.1007/s00359-006-0096-7

Von der Emde G, Bleckmann H (1998) Finding food: senses involved in foraging for insect larvae in the electric fish *Gnathonemus petersii*. J Exp Biol 201:969–980

Von der Emde G, Ringer T (1992) Electrolocation of capacitive objects in four species of pulse-type weakly electric fish I. Discrim Perform Ethol 91:326–338. doi:10.1111/j.1439-0310.1992.tb00873.x

Von der Emde G, Schwarz S (2002) Imaging of objects through active electrolocation in *Gnathonemus petersii*. J Physiol Paris 96:431–444. doi:10.1016/S0928-4257(03)00021-4

Wallace RA, Selman K (1981) Cellular and dynamic aspects of oocyte growth in teleosts. Am Zool 21:325–334. doi:10.1093/icb/21.2.325

Westby GWM, Kirschbaum F (1982) Sex differences in the waveform of the pulse-type electric fish, *Pollimyrus isidori* (Mormyridae). J Comp Physiol 145:399–403. doi:10.1007/BF00619344

Zakon HH, Lu Y, Zwickl DJ, Hillis DM (2006) Sodium channel genes and the evolution of diversity in communication signals of electric fishes: convergent molecular evolution. PNAS 103:3675–3680. doi:10.1073/pnas.0600160103